ELSEVIER

Research Article

Local gene density predicts the spatial position of genetic loci in the interphase nucleus

Andrea E. Murmann[a,b], Juntao Gao[c], Marissa Encinosa[a], Mathieu Gautier[d], Marcus E. Peter[e], Roland Eils[c], Peter Lichter[b,*], Janet D. Rowley[a]

[a]Department of Medicine, Section Hematology/Oncology, University of Chicago, Chicago, IL 60637, USA
[b]Division of Molecular Genetics, Deutsches Krebsforschungszentrum, Im Neuenheimer Feld 580, 69120 Heidelberg, Germany
[c]Theoretical Bioinformatics Division, Deutsches Krebsforschungszentrum, 69120 Heidelberg, Germany
[d]Institut National de la Recherche Agronomique, Jouy en Josas, 78352 Cedex, France
[e]The Ben May Institute for Cancer Research, University of Chicago, Chicago, IL 60637, USA

Abstract

Specific chromosomal translocations are hallmarks of many human leukemias. The basis for these translocation events is poorly understood, but it has been assumed that spatial positioning of genes in the nucleus of hematopoietic cells is a contributing factor. Analysis of the nuclear 3D position of the gene *MLL*, frequently involved in chromosomal translocations and five of its translocation partners (*AF4*, *AF6*, *AF9*, *ENL* and *ELL*), and two control loci revealed a characteristic radial distribution pattern in all hematopoietic cells studied. Genes in areas of high local gene density were found positioned towards the nuclear center, whereas genes in regions of low gene density were detected closer to the nuclear periphery. The gene density within a 2 Mbp window was found to be a better predictor for the relative positioning of a genomic locus within the cell nucleus than the gene density of entire chromosomes. Analysis of the position of *MLL*, *AF4*, *AF6* and *AF9* in cell lines carrying chromosomal translocations involving these genes revealed that the position of the normal genes was different from that of the fusion genes, and this was again consistent with the changes in local gene density within a 2 Mbp window. Thus, alterations in gene density directly at translocation junctions could explain the change in the position of affected genes in leukemia cells.
© 2005 Elsevier Inc. All rights reserved.

Keywords: MLL; Translocation; Nuclear organization; Gene density

Introduction

Chromosomal aberrations are found in all types of human cancer. Specific recurring chromosome aberrations, such as certain translocations, are often associated with a particular type of leukemia, lymphoma or sarcoma and may be a cause of cellular transformation [1]. However, the molecular mechanisms of a translocation event are generally unknown. Most chromosomal translocations are the result of reciprocal exchange of large chromosomal segments, typically between two different chromosomes. After a double strand break

event in each participating chromosome, derivative chromosomes are generated by fusion. This can result in chimeric genes at the fusion points that code for hybrid proteins with altered functions, which might cause malignant transformation [2]. One such gene is *MLL* (*m*ixed-*l*ineage *l*eukemia or *m*yeloid-*l*ymphoid *l*eukemia), which can be fused to one of approximately 60 possible other genes. The respective translocation partner is characteristic for the type of leukemia [3]. The *MLL* gene was initially identified and cloned in 1991 from translocations that involved chromosome band 11q23 [4]. The most common translocation partners of *MLL* seen in human leukemia are *AF4*, *AF6*, *AF9*, *AF10*, *ENL* and *ELL*, located on chromosome bands 4q23, 6q27, 9p23, 10p12, 19p13.3 and 19p13.1, respectively. Translocations

---

t(4;11), and t(11;19)(q23;p13.3) are found primarily in acute lymphoblastic leukemia and t(6;11), t(9;11), t(10;11) and t(11;19)(q23;p13.1) predominantly in acute myeloblastic leukemia. The propensity of the *MLL* gene to rearrange, and the diversity of the partner genes that fuse to *MLL*, has made it difficult to postulate a common mechanism to explain the pathogenic role of the fusion transcripts. Although there are models attempting to explain how *MLL* recombines molecularly with its translocation partner genes [5], it is virtually unknown how recombination occurs in the context of chromosome organization in the cell nucleus. The neighborhood of certain chromosomes or genes could very well affect the probability of a reciprocal exchange, and it has been suggested that the respective genes are spatially close in the hematopoietic precursor cells, where the translocation occurs [6].

While the determinants of the spatial localization of genes in the nucleus are still a matter of investigation, several features have emerged. An initial study reported that genes are preferentially located at the periphery of chromosome territories [7]. Subsequent analyses confirmed this observation and revealed additional features such as differential intra-chromosomal gene positioning within one gene family [8].

In some special cases of highly expressed genomic segments, genes were even observed to extend away from chromosome territories [9–11]. Furthermore, gene specific positioning was detected with regard to the orientation towards the nuclear interior [7,12]. However, more recently, it was also reported that certain genes are not necessarily located at the periphery of chromosomes or the surface of subchromosomal domains [13].

Gene density and chromosome size were described to be factors that determine the localization of entire chromosomes within the nucleus [14–19]. It is unknown, however, in how far gene density of smaller chromosome regions also correlates with their positioning in relation to the nuclear radius. It is tempting to hypothesize that, for the proper prediction of the localization of individual genes and loci, one might have to consider not only the gene density of entire chromosomes, the gene density of chromosomal arms or chromosomal subdomains, but also the DNA composition in the immediate chromosomal neighborhood of genes or the local environment. *MLL* and its various translocation partners provide a unique system to study such a model and the effects of a change in local gene density caused by the translocation on the 3D position of a locus within the nucleus.

We now demonstrate that *MLL* as well as genes, which frequently fuse to *MLL*, localize in defined radial zones in the 3D space of the interphase nucleus of hematopoietic cells. These localizations are tissue-specific but species-independent. Upon reciprocal translocation, partner genes change 3D localization in a reproducible and predictable fashion. Analyses of global and local gene densities allowed us to postulate a model in which the gene density within a region of about 2 Mbp surrounding a locus determines the 3D localization of genes.

Materials and methods

Cells and tissue culture

Primary human bone marrow cells (CD34$^+$ and CD33$^+$) were purchased from AllCells Inc. (Berkeley, CA). Chinese muntjac fibroblasts, isolated from tissue of a stillbirth Chinese muntjac fawn provided by the University of Bielefeld, Department of Animal Behavior, were prepared by Dr. M. Scheuermann and propagated as described elsewhere [20]. The female Indian muntjac cells were a gift of Dr. Roger A. Schulz, UT Southwestern Medical Center, Dallas. The male human dermal fibro-blasts (HDF) derived from foreskin and the muntjac fibroblasts were grown in Dulbecco's modified Eagles medium (DMEM) containing 10% (v/v) fetal calf serum (FCS), 1.0 mg/L-glucose, 2 mM L-glutamine and 100 U/ml penicillin/100 μl/ml streptomycin. Jurkat T cells (clone E6-1), MonoMac6, MV4–11, NALM6, Raji, SKW6.4, THP-1, 11365 (B lymphoblastoid cell line, Cytogenetics laboratory, University of Chicago) and U-937 cells were grown in 90% RPMI 1640, 10% FBS, 100 U/ml penicillin/100 μg/ml streptomycin. RS4;11 cells were grown in Iscove's modified Dulbecco's medium, 10% FBS, 100 U/ml penicillin/100 μg/ml streptomycin. All cells were cultured at 37°C and 5% CO_2. In all cell lines with the translocations affecting *MLL*, the translocation was verified by FISH (data not shown). For 3D-FISH analysis, fibroblasts were grown on glass slides to 80% confluency. Prior to paraformaldehyde (PFA) fixation to preserve the 3D nuclear structure, suspension cells were resuspended in 37°C warm PBS to 0.5–1 million/ml. 0.5 ml cell suspension was placed on poly-L-lysine a coated Poly-Prep Slides™ slide (Sigma). For 5 to 10 min, the cells were allowed to attach to the surface, while a Press-to-Seal™ silicon isolator (20 mm diameter, 1.0 mm deep, Molecular Probes) prevented the suspension to disperse on the slide.

3D fixation

In order to preserve the three-dimensional structure of interphase cell nuclei, the specimen was fixed and permea-bilized according to protocols reported elsewhere [7,21]. After a wash in PBS, cells were fixed in 4% PFA/PBS for 12 min. Permeabilization to facilitate probe penetration was achieved by incubation of the specimen with 0.5% (w/v) saponin/0.5% (v/v) Triton X-100/PBS for 20 min followed by three washes with PBS. After equilibration in 20% glycerol/PBS for 30–60 min, specimens were subjected to three cycles of freeze-thawing (primary cells were frozen only once to minimize cell loss). Specimens were stored at −80°C. Slides were thawed at room temperature then washed three times in PBS and incubated in 0.1 M HCl for 5–15 min (optimized for each cell type) followed by a final wash in PBS prior to denaturation.

FISH probes

Human BAC clones were purchased from BACPAC Resources Center (Oakland, CA) and Invitrogen (Carlsbad, CA). Various loci and genes were detected by fluorescence in situ hybridization (FISH) using the following genomic probes: for the human cell lines MonoMac6, MV4–11, RS4;11 and THP-1, the *MLL* probe from Vysis was utilized that delineates the split of *MLL*. In cell lines with normal *MLL*, the clone RP11-770J1 was used to detect the entire gene; *AF4*: CTD-2505N20 and CTD-2574C18; *AF9*: CTD-2177K11 and CTD-3005E18; *ENL*: RP11-819E16, *ELL*; 19468 and 29473 (gift of Dr. M. Thirman, University of Chicago, IL). CASP8 and -CASP10: BAC cl.43 (gift of Dr. J. Lahti, St. Judes-Hospital in Memphis), STS Marker D2S163: RP11-53G6.

Genomic DNA of cattle BAC clones with the ID number 0809B10 (*MLL*), 0494F04 (*AF4*) and 1086D03 (*AF9*) were isolated from the INRA bovine BAC library using relevant bovine-specific primers for each gene considered as previously described [22]. Genomic clones were labeled by nick translation with derivative nucleotides biotin-16-dUTP, digoxigenin-11dUTP, estradiol-15-dUTP (all Roche) or DNP-11-dUTP (PerkinElmer).

Fluorescence in situ hybridization

Preparation of metaphase chromosome spreads and hybridization to these samples were performed as described elsewhere [21]; 3D-FISH was performed as previously described [7]. 200 ng of gene-specific-labeled probe for FISH on metaphase cells and 600 ng probe for 3D-FISH were precipitated with 5 μg of human Cot-1 DNA (on human specimen) or 5 μg of cattle Cot-1 DNA (Bovine hybloc, Applied Genetics Labs, Foster City, CA) together with 10 μg of sonified Chinese muntjac DNA (on muntjac specimen). The probes were resolubilized in 12 μl hybridization buffer (50% deionized formamide/10% dextran/2× SSC). When custom-made probes were combined with a commercial probe, the precipitated DNA was resuspended with 3.2 μl of the commercial probe and 8.4 μl of the LSI/WCP hybridization buffer (Vysis). Hybridization was performed at 37°C for 48 h (3D-FISH). Washes and detection of hybridized probe were performed as previously described [23] with a final washing stringency of 2× SSC/pH 7.0. To prevent unspecific antibody binding, the slide was blocked for 20 min with a blocking buffer (4× SSC/4% (w/v) BSA). Biotinylated probes were detected using 5 μg/ml Cy5-streptavidin (Jackson ImmunoResearch Laboratories, West Grove, PA), digoxigenin-labeled probes with mouse-anti-digoxigenin-Cy3 or -Cy5 antibody (Jackson Immuno-Research Laboratories), and DNP-labeled probes were detected with 4 μg/ml rabbit-anti-DNP and 3 μg/ml goat-anti-rabbit-IgG-F(ab′)2-flourescein isothiocyanate (FITC) or -Cy5. Following incubation at 37°C for 45 min, slides were washed at 42°C in 4× SSC/0.05% (v/v) Tween-20. Coverslips were mounted using Vectashield with DAPI (Vector, Burlingame, CA). The probes were tested by FISH on metaphase chromosomes prior to hybridization on 3D preserved specimens.

Imaging

Microscopic images of metaphase chromosomes were acquired with a cooled CCD camera system Model SenSys Series 200 from Photometrics LTD (Tucson, AZ) mounted on an epifluorescence microscope (Axioplan, Carl Zeiss, Oberkochen, Germany). IPLab software was used to capture the images and to export them in .tif format. The images were further enhanced using the computer program Adobe Photoshop 6.0.1.

For the acquisition of confocal image stacks, a Leica SP2 AOBS spectral laser scanning confocal microscope was used, which was operated with the software LCS 2.5v1347. The Leica DMIRE2 (inverted) microscope was equipped for conventional epifluorescence (50 W Hg) and DIC optics. The images were captured with a 63× NA 1.4 oil immersion lens. For simultaneous four-color detection, the following laser lines were used: 488 nm (FITC), 543 nm (Cy3), 633 nm (Cy5) and 405 nm (DAPI and DIC). The signals of DNA counterstain and up to 4 different genomic loci were recorded in separate channels. The pinhole for all scans was kept constant at 1 Airy. All 3D image stacks of fixed cells were acquired with steps between 0.2 μm and 0.5 μm in *z*-directions. Preferably, the same step increments were used for each experimental series. The image resolution was 512 × 512 pixels. If two or more fluorochromes were imaged, the modus "sequential scan" was used. The detection spectrum of the fluorochromes was adjusted to have as little overlap as possible. In the majority of the scans, the color order during acquisition was the following: Cy3, FITC, Cy5, DAPI including DIC. To improve the signal to noise ratio, all images were averaged 6 or 8 times. To delineate the shape of the nucleus and the cell, a differential interference contrast (DIC) image was acquired.

Image processing and 3D analysis

3D surface reconstruction of gene signals were performed using the computer program Amira 3.1 (Eurostart Services, Düsseldorf, Germany). Distances between gene signals to the nuclear surface and to the nuclear center were calculated with the help of the 3D computational tools described [24]. Briefly, after importing the confocal image stacks into Amira 3.1, the coordinates of the nuclear surface and of each gene signal were exported into separate files (IV format), which were used for calculations within the software application. The IV-file contained all *x*, *y* and *z* coordinates of the created surface points of either a gene

signal or the nucleus. To assess the position of, e.g. a gene in a nucleus, 3 IV-files were created, one for the nuclear counterstain and two for each gene signal. The position of a gene signal in the 3D space was sufficiently described by the position of its geometric center. An algorithm was designed to calculate the x, y and z coordinates of its geometric center for the IV-file. For the details of the calculation, see [24]. The geometric center of the nucleus was chosen as the reference point. In order to compare different signals recorded in different experiments and in nuclei of different cells, a mathematically defined method was developed, which allowed assessment of the position of genes in the nucleus relative to the nuclear periphery and the nuclear center. The nuclear radius (which was summed up as the distance of the signal to the nuclear center plus the distance to the nuclear periphery) was divided into 5 equal parts resulting in 5 shells of identical depth (Supplementary Fig. 1). To determine the distance between a gene and the nuclear surface, the program identified the nearest surface point to geometric center of the gene. Due to the difference in geometry of fibroblast nuclei (oval and flat), the shell analysis method used for hematopoietic cells could not be applied to fibroblasts. Therefore, in fibroblasts, the distances of the genes to the geometric center of the nucleus were compared.

Results

Genes in hematopoietic cells have a highly characteristic spatial position

The spatial analysis of gene loci was performed in three-dimensionally preserved cell specimen after co-visualization by FISH, and the subsequent analysis of confocal images utilizing dedicated software applications was as described in the Materials and methods section. The topology of *MLL* was analyzed in different hematopoietic cell types: primary CD34$^+$ and CD33$^+$ cells isolated from human bone marrow obtained from normal individuals, the 11365 cell line representing cells with a normal karyotype, and Nalm-6, SKW6.4, as well as Jurkat cells all with an abnormal karyotype but a normal chromosome 11. In contrast, Raji and U937 cells have various abnormalities with either deletion or inversions of chromosome 11 but not involving the *MLL* gene. An example of a rendered nucleus after 3D-FISH is illustrated in Fig. 1A, and the location of the 5 concentric shells is shown in Fig. 1B. The analysis revealed that *MLL* is generally located in the second outer shell of the nucleus in all tested cell types (Fig. 1C), and the nuclear distribution appeared independent of the constitution of chromosome 11.

Comparative analysis of the positions of *MLL* and its potential translocation partner genes was performed in the cell line 11365 (Fig. 2) and in a subset of CD34-positive and

CD33-positive cells (*MLL*, *AF4*, *AF9*, not shown). In all three cell types, the same nuclear distribution pattern was observed. In 11365 cells, *MLL*, *AF4*, *AF6*, *AF9*, *ENL*, *ELL* and two control loci (*D2S163*, *CASP8/CASP10*) were analyzed in 5 different experiments (Fig. 2A). The control loci were chosen from chromosome 2 since the subbands 2q33 and 2q35 have not been reported to translocate with *MLL* or 11q23 in leukemia.[1] Statistical analysis revealed that each gene and chromosomal locus showed a characteristic distribution pattern in the interphase nucleus, with the locus *D2S163* on 2q35 located in the most exterior and the genes *ENL* and *ELL* on 19p13 in the most interior nuclear shell. Interestingly, the mean distance of the three most common translocation partners, *AF6*, *AF9* and *AF4*, to the nuclear surface was remarkably similar. While they tended to localize to a position more peripheral than *MLL*, the median position for all three genes clustered at the border of shells one and two.

The 3D position of genes is conserved across different species

To determine whether these characteristic gene positions were specific for cell type and/or species, we extended the analysis to human fibroblasts and fibroblasts from two closely related species of deer, *Muntiacus muntjak* and *Muntiacus reevesi*. Indian muntjac which has the lowest number of chromosomes known in mammals ($2n = 6/7$), and Chinese muntjac ($2n = 46$), are distant enough from humans but sufficiently closely related to each other to generalize the findings. *MLL*, *AF4* and *AF9* were detected using fluorescently labeled probes (Fig. 3). In *M. muntjak* *MLL*, *AF4* and *AF9* are on chromosomes 2q36-q38, 1p12-p13 and 3q39, respectively, while, in *M. reevesi* *MLL*, *AF4* and *AF9* are on chromosomes 10, 21 and 19, respectively (Supplemental Fig. 2). As outlined in the Materials and methods section, the distances of the genes to the geometric center of the nucleus were measured. The distribution pattern in the fibroblasts of the three species was different from the pattern found in 11365 cells analyzed in the same way (data not shown). In all fibroblasts, *MLL* had the largest median distance to the nuclear center, whereas *AF4* and *AF9* displayed a similar but shorter distance. This is in contrast to the distance of *MLL* to the nuclear center in 11365 cells, which was on average the shortest. These results provide evidence for a difference in the nuclear localization of genes between hematopoietic cells and fibroblasts on one hand and for a cell-type specific pattern conserved across mammalian species on the other hand consistent with previous reports [15,26].

---

[1] Searches of the Mitelman Database of Chromosome Aberrations in Cancer revealed that t(2;11)(q33;q23) has only been described once in the analysis of tumors of the nasal cavity and paranasal sinuses [25]. So far, a t(2;11)(q35;q23) has not been described anywhere.
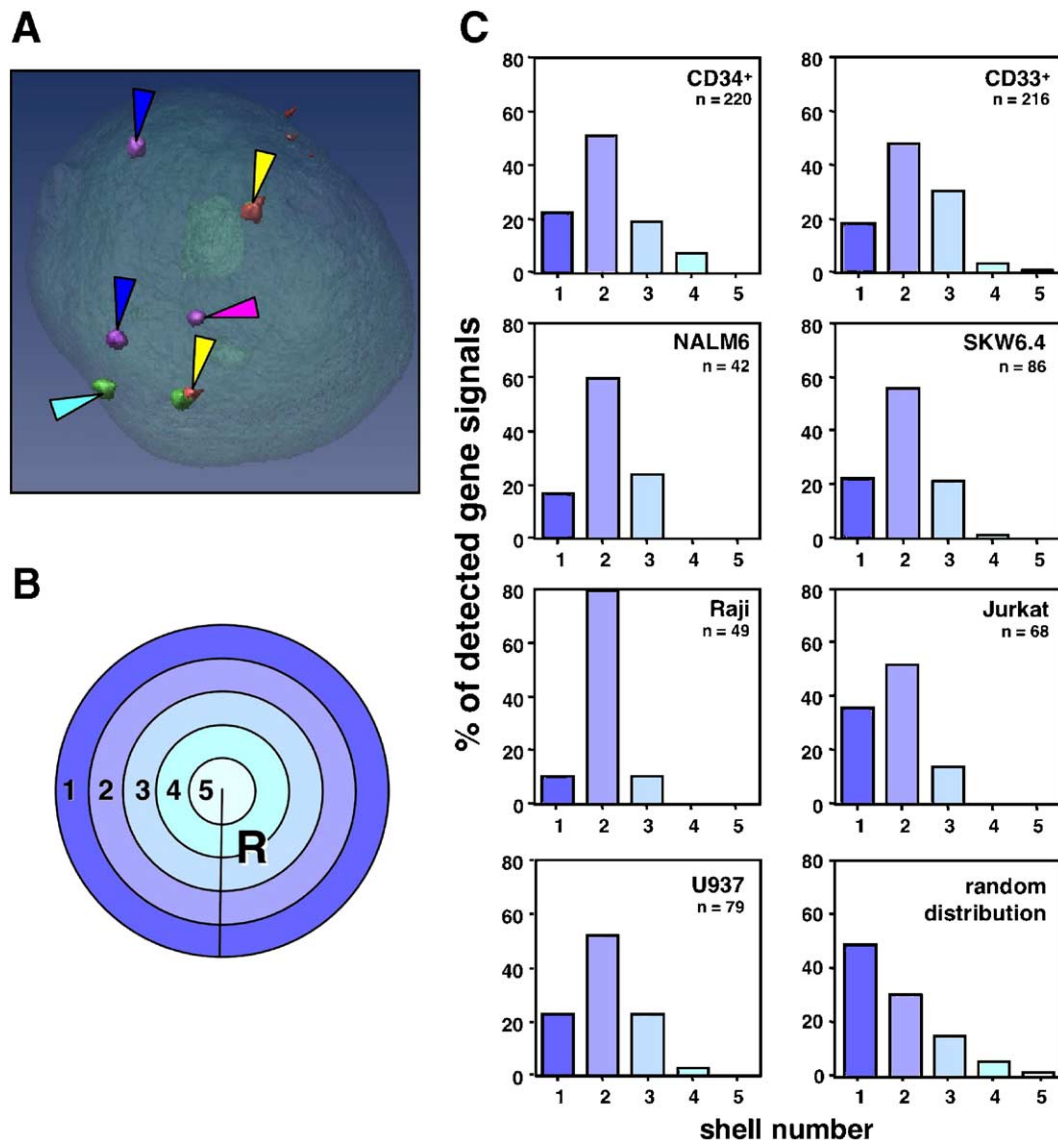
Fig. 1. *MLL* has a characteristic 3D localization in various hematopoietic cells. (A) 3D reconstruction of 1 nucleus after 3 color FISH. Surface rendered MonoMac6 cell nucleus from confocal image stacks of PFA-fixed interphase nuclei using the Amira 3.1 computer program. Blue arrow head: *AF9* on chromosome 9; yellow arrow head: 5′*MLL* and 3′*MLL* on chromosome 11; pink arrow head: 5′*AF9* and 3′*MLL* on der(9); aqua arrow head: 5′ *MLL* on der(11). (B) Schematic display for the analysis of the 3D position of *MLL* using shells of equal radius division. (C) Analysis of the 3D position of *MLL* in various cells and cell lines. Nalm-6, SKW6.4, Raji, Jurkat and U937 are cell lines. CD34$^+$ and CD33$^+$ cells were primary hematopoietic stem cells and myeloid cells, respectively, (purchased from AllCells, LLC., CA) isolated from bone marrow with a MACS kit, purity of >90%. *n* = number of analyzed genes. A list of the analyzed gene signals and cell lines is provided in Supplementary Table 1. An assumed random distribution of genes is shown in the bottom right panel.

Translocation events can change the 3D localization of genes

In order to assess the effect of a translocation on the 3D position of rearranged genes, we analyzed the position of fusion genes of translocation t(9;11) in the cell lines Mono-Mac6 (Fig. 4) and THP-1 and of translocation t(4;11) in the cell lines MV4–11 and RS4;11 (Fig. 5). In both cell lines with t(9;11), the normal *AF9* gene preferentially localized peripheral to the *MLL* gene, the rearranged *AF9/MLL*(3′) gene was distributed in the outer shells corresponding to the normal *MLL* gene topology, and the *MLL* (5′) portion on the derivative

chromosome 11 was positioned similar to the normal *AF9* gene, while the truncated *AF9* gene on the derivative chromosome 9 in the two lines differed in the shell position (Figs. 4B and 5A). Notably, the derivative chromosome 9 was differently rearranged in the two monocytic lines as the der(9) chromosome in the THP-1 cell line has an additional inversion.

Both the pro B-cell line RS4;11 and the monocytic cell line MV4–11 harbor the translocation t(4;11) leading to an *MLL-AF4* fusion gene. Again, the normal *AF4* gene localized preferentially closer to the nuclear surface than the normal *MLL* gene, while the position of the two fusion genes *AF4-MLL* and *MLL-AF4* on the derivative chromo-
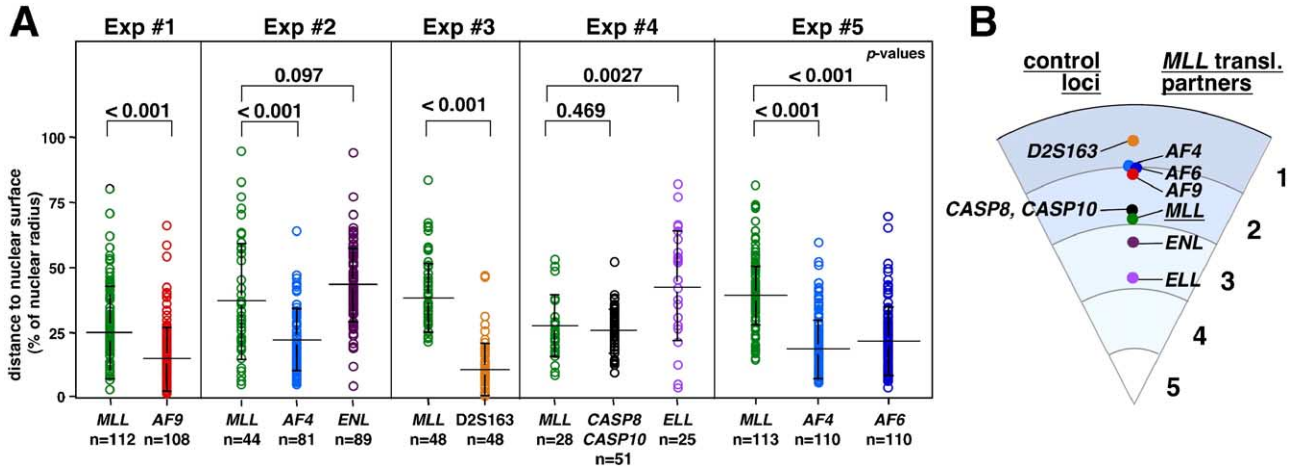
Fig. 2. Comparison of the position of various genes in 3D fixed nuclei of 11365 cells. (A) Analysis of the 3D position of genes using shells as displayed in Fig. 1B. All cells were PFA-fixed, and 3D-FISH was performed. The combination of FISH probes was performed with the *MLL* clone as a reference. The mean positions of each gene were normalized to the position of *MLL* in each experiment and plotted. Values for standard deviation and significance (*P* value, Student's *t* test). *n* = number of analyzed genes. (B) Summary of the shell localization of all genes shown in panel A, after normalizing the distances to the position to *MLL* in each experiment.

somes 4 and 11, respectively, occupied shell positions between the normal *AF4* and *MLL* genes (Figs. 5B and C).

Thus, the intact gene copies were distributed in the same way as in cells with normal karyotype, while the topologies of similarly altered genes were very similar. Since hematopoietic cell lines of different lineage exhibited the same distribution pattern for the respective rearranged genes, this topological feature seemed to be cell-type-independent.

Gene density in the immediate proximity of genes is associated with their 3D localization

Our findings are not consistent with the model of the nuclear position of entire chromosomes based on their gene

density (see Introduction). Accordingly, we analyzed the relationship of gene topology and gene density on several levels of subchromosomal regions. To this end, we assessed the gene density of whole chromosomes, chromosomal arms and segments of 0.2, 1, 2, 5, 10, 20 and, when possible, 30 and 40 Mbp surrounding the tested loci on normal and derivative chromosomes (Supplementary Fig. 3 and data not shown) for the genes *MLL*, 5 of its potential translocation partners as well as two control loci in the cell line 11365 (Fig. 6). As the genes *AF4*, *AF6*, *AF9* and *MLL* map on chromosomes with similar gene density, the more central positioning of *MLL* does not fit the view of the role of gene density of entire chromosomes. The same is true for the differences observed for pairs of genes between chromosomes 2 and 19 (Fig. 6). The best association with the nuclear shell position was found for the gene density of a region of 1 Mbp upstream and downstream (2 Mbp window) of a locus (Fig. 6C).

Association of the 2 Mbp window of gene density was also strongest, when analyzing translocation breakpoints, which resulted in the change of nuclear shell positions. Fig. 7 shows the analysis of the t(9;11) translocation in MonoMac6 cells (panel A) and the analysis of the t(4;11) translocation in RS4;11 cells (panel B). The gene density around the loci on der(9) and der(4) was higher than on der(11), and the locus position changed accordingly. In Fig. 7C, the result of a published analysis of cells with a t(11;22) translocation involving the genes *EWSR1* on chromosome 22q12 and *FLI1* on chromosome 11q24, for which a positional shift of the derivative genes was observed [27], was analyzed in the same way. The published median distance of genes to the nuclear center was converted to the distance to the nuclear periphery. Again, the fused genes occupied an intermediate shell position, when compared to the gene copies on normal chromosomes (Fig. 7C). Thus,
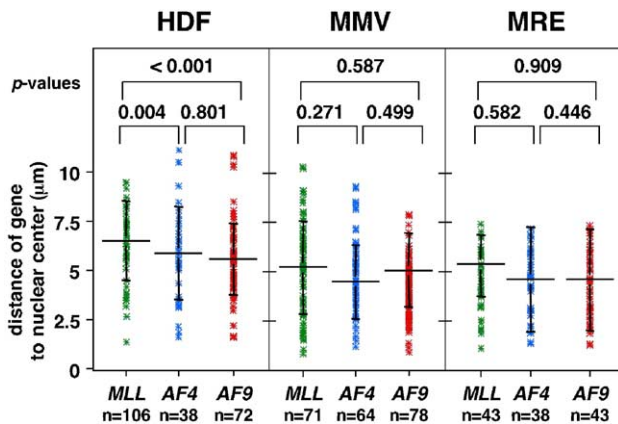

Fig. 3. Comparison of the 3D positions of *MLL*, *AF4* and *AF9* relative to the nuclear center in fibroblast nuclei from different species. Distance measurements of *MLL* to nuclear center in HDF (human dermal fibroblasts), MMV (Indian muntjac fibroblasts), MRE (Chinese muntjac fibroblasts). Values in micrometer. *n* = number of measurements. Values for standard deviation and significance (*P* value, Student's *t* test). Green = *MLL*, blue = *AF4*, red = *AF9*.
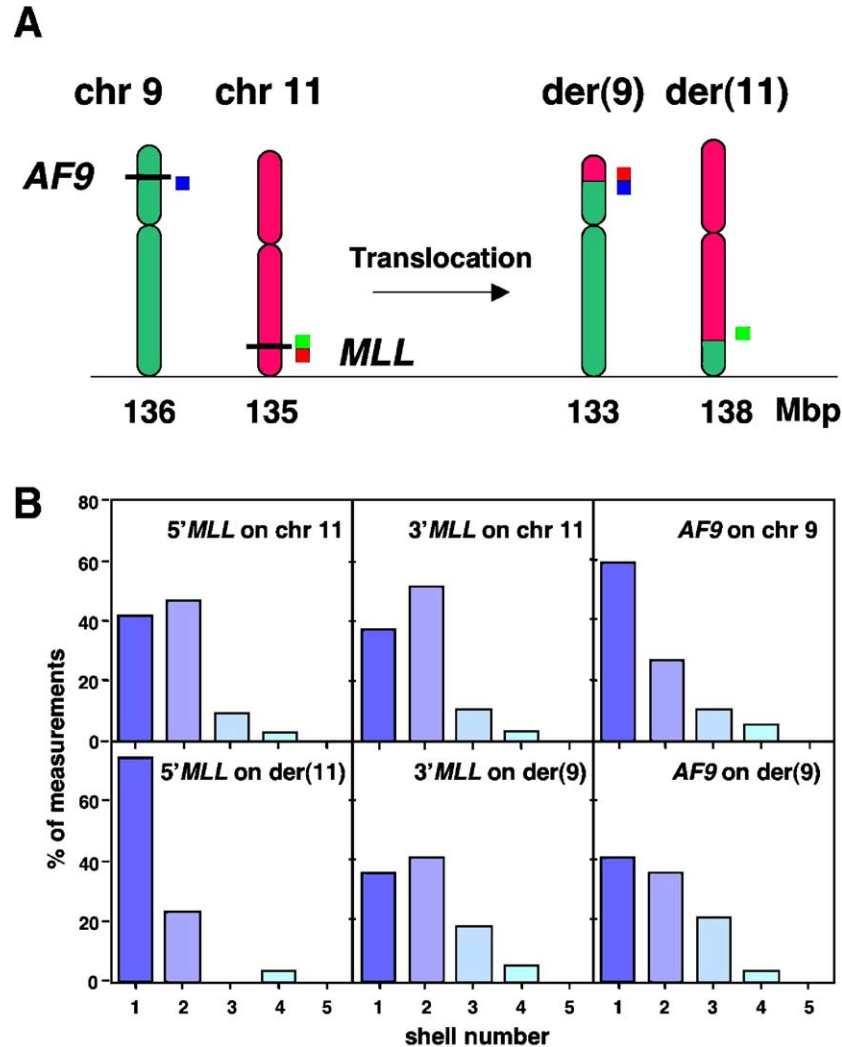
Fig. 4. After translocation, the 5′MLL and 5′AF9 regions acquire the 3D positions of each other prior to the translocation in MonoMac6 cells. (A) Change of size after translocation between chromosome 9 and 11. Purple line indicates relative position of the genes AF9 and MLL. Colored bars to the left of each chromosome indicated the position of FISH clone allowing to identify each color combination in the interphase nucleus. Blue for 5′AF9, green for 5′MLL, red for 3′MLL. Blue for normal 9, red/green for normal 11, red/blue for der(9), green for der(11). (B) Distribution of 5′MLL, 3′MLL and AF9 on normal and derivative chromosomes relative to nuclear surface. Upper panels: positions of genes on normal chromosomes. Lower panels: positions of genes in derivative chromosomes. Positions were analyzed using shells of equal radius division as described in Supplementary Fig. 1. $n = 40$ cells were evaluated. The 5′ and the 3′MLL probes on the normal chromosomes 11 gave a similar result. The 3′MLL probe, detecting the translocated part of MLL on der(9), maintained the shell position of the normal MLL gene. The 5′AF9 probe, which detects the part of AF9 on the der(9), showed a shell position similar to 3′MLL on the der(9). The 5′MLL probe, which detects the part of MLL on the der(11), changed shell position to that of AF9 on chromosome 9.

the gene density in the immediate vicinity of a gene (a region as small as 2 Mbp) correlates well with its 3D localization in the interphase nucleus.

Discussion

In an attempt to find principles that determine the nuclear localization of genes, the spatial position of MLL and five of its potential translocation partner genes was analyzed in various human hematopoietic cell lines and primary cells as well as primary human and muntjac fibroblasts. To be able to describe the position of a gene in the interphase nuclei

most accurately, all the data obtained for this paper combined 3D specimen preservation [7], precise 3D image reconstruction of confocal image stacks and 3D calculation of distances within the reconstructed nuclei.

In contrast to the studies which performed the bulk of their analyses in 2D fixed cells with only a few 3D experiments to confirm the data [10,11], all analyses in this work were exclusively performed on 3D fixed nuclei. The general fixation method for 2D-FISH involves a hypotonic treatment, methanol-acetic acid dehydrating fixation and ultimately dropping of the fixed cell material on a slide resulting in flattened nuclei suitable for 2D analysis. This hypotonic treatment causes an enlargement of cells and their

nuclei and the chromatin to be more loosely packed [28,29] making distance measurements between genes inaccurate. Another disadvantage of the 2D analysis is the possibility of misinterpretation of images. Genes that would be located on top of each other in a spherical nucleus (e.g. of a hematopoietic cell) can appear to be in close proximity. To compensate for these problems, Roix et al. analyzed several thousand cells using a semi-automated high-throughput image acquisition system to find significant differences in gene positions [6]. Kozubek and coworkers

developed a prediction model to interpret the maximum image of fixed material (after MAA or PFA fixation), which is the projection of all confocal images acquired for one nucleus, and calculated the theoretical distribution of loci [30]. This method allowed the automated analysis of the FISH-painted nuclei and a high-throughput manner.

We chose the established 4% paraformaldehyde fixation method to preserve the nucleus' 3D structure [7,21] with a few modifications to optimize analysis in different cell lines. It is the fixation method that has repeatedly been shown to adequately conserve the chromatin architecture during FISH [7,31].

The position of genes in the 3D space of the interphase nucleus was determined with the help of 3D-reconstructed confocal image stacks and specifically designed computational tools [24] to determine the distances among genes and the position relative to the nuclear radius. We expressed the 3D gene positions as percent of the nuclear radius, and genes were assigned to the volume of concentric shells of equal volume, analogous to a 2D system that was published earlier [14,32]. There, the 2D area of the nucleus was divided into 5 concentric rings of equal area.

The normal gene copies of *MLL*, *AF4*, *AF6*, *AF9*, *ELL* and *ENL* were found characteristically distributed in nuclear shells. Their distribution was the same in cells of different hematopoietic origin. Furthermore, in leukemic cells, where one gene copy was rearranged, the remaining normal locus was positioned as in cells with normal karyotype. Most interestingly, rearranged genes changed their nuclear shell positions. The same fusion gene (t(9;11) or t(4;11)) in different cell lines displayed the same topology. Since hematopoietic cell lines of different lineage exhibit the same distribution pattern for the respective rearranged genes, this topological feature seems to be cell-lineage-independent. There was a difference in the nuclear localization of genes between hematopoietic cells and fibroblasts, suggesting tissue-specific differences of gene positioning consistent with previous reports [26,33]. 3D analysis from human and two muntjac species revealed a high evolutionary conservation suggesting that a cell-type-specific gene positioning in the nucleus is conserved across mammalian species. A high
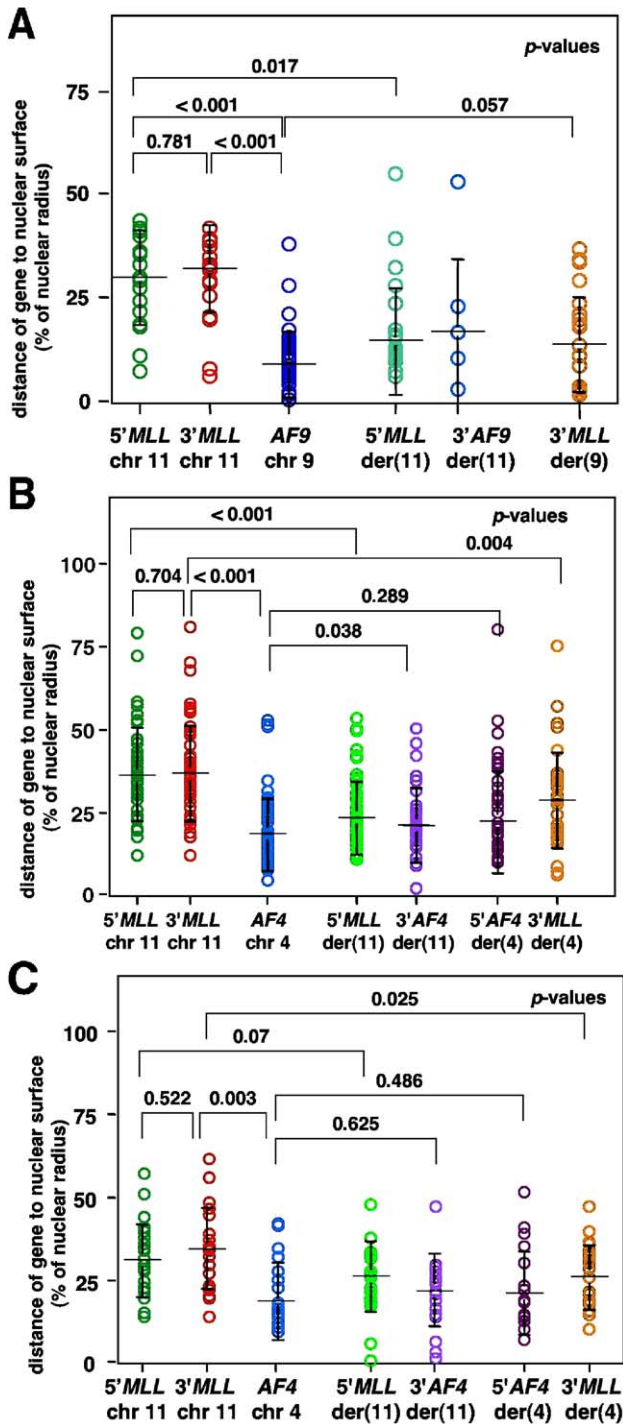
Fig. 5. Changes in 3D positions of genes following translocation events. (A) Following translocation, the 5′*MLL* and 5′*AF9* regions acquire the 3D positions of each other prior to the translocation in THP-1 cells. Positions of the 5′*MLL*, 3′*MLL*, 5′*AF9* and 3′*AF9* signals relative to the nuclear surface. 18 cells were analyzed. Some signals for the derivative chromosomes could not clearly be identified, resulting in fewer measurements. (B) Following translocation, both the 5′*MLL* and 5′*AF4* regions acquire the 3D position and distance to the nuclear surface that lies between the location of *MLL* on chromosomes 11 and *AF4* on chromosome 4 in the B-cell line RS4;11. Positions of the 3′*MLL*, 5′*MLL*, 3′*AF4* and 5′*AF4* signals relative to the nuclear surface. P values were calculated with the computer program Excel. (C) After translocation, both the 5′*MLL* and 5′*AF4* regions acquire the 3D position of *AF4* in the monocytic cell line MV4–11. Position of 5′*MLL*, 3′*MLL*, 3′*AF4* and 5′*AF4*, relative to nuclear surface. *n* = 25 cells were evaluated. In 10 nuclei, not all the signals for the derivative chromosomes were identifiable. der = derivative chromosome.
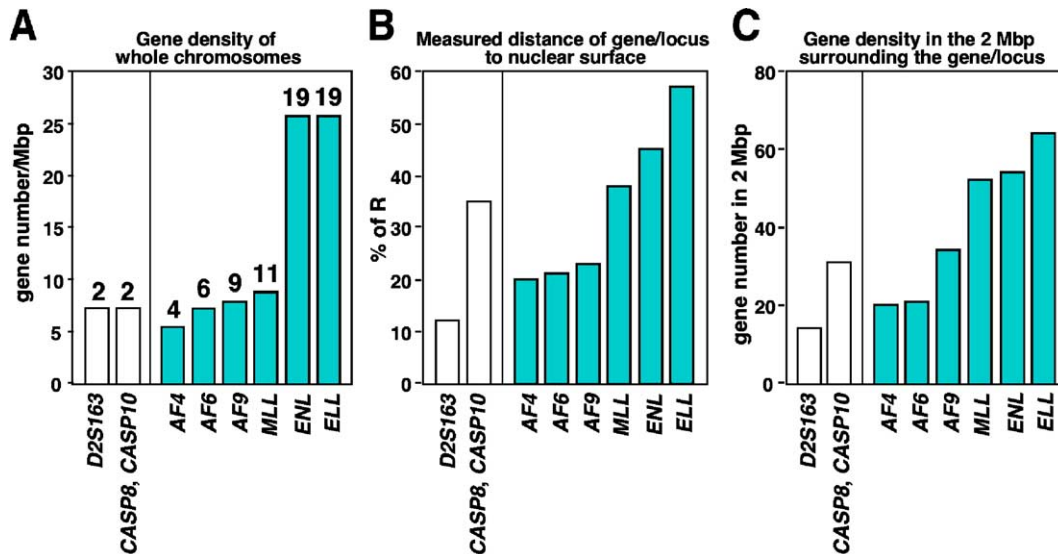
Fig. 6. Comparison of the gene density of entire chromosomes with the local gene density within 2 Mbp of genes/loci for being predictors for the 3D nuclear position of genes. Light blue bars are relevant for the control loci, dark green bars for *MLL* and 5 translocation partners. (A) Gene density of entire chromosomes. (B) Measured distances of genes/loci to nuclear surface. Values are the normalized median values. (C) Gene density in the 2 Mbp windows surrounding the genes/loci. Gene density information for the human chromosomes was obtained from the website http://www.ncbi.nlm.nih.gov/mapview/maps.cgi.

conservation between species has previously been reported for intraterritory gene positions between human and mouse [11,13]. The factors that determine the relative positions of chromosomes within the nucleus are not fully understood. There seems to be a correlation between the estimated gene density (number of genes per Mbp) of each chromosome and its average position within the nucleus. The estimated gene density of each chromosome has been correlated with its average position within the nucleus. Chromosomes with fewer genes are often associated with the nuclear periphery, while gene-rich chromosomes reside in a more internal nuclear position [14,19]. While this is true for (proliferating) spherical nuclei, such as in hematopoietic cell lines, in quiescent nuclei, chromosomes often appear to be positioned according to their size [16–18,32]. Controversy remains over the positioning of chromosomes in non-spherical nuclei, such as in fibroblasts. Boyle et al. found chromosomes in proliferating human dermal fibroblasts to be organized by gene density [19]. In contrast, Bolzer et al. reported that in fibroblasts chromosomes are positioned by size, even in proliferating nuclei [17].

The connection between gene density and localization was also evident in a comparison of the localization of human chromosomes 18 and 19 and their derivatives generated by reciprocal translocation. While similar in size, chromosome 19 is highly gene-dense, whereas chromosome 18 is relatively gene-poor. In nuclei of normal cells, the chromosome 19 territory had a more internal position than chromosome 18 [14]. Whether translocation events can change the positions of chromosomal domains has previously been tested by analyzing chromosome rearrangements between or involving human chromosomes 18 and 19 [14,15]. Translocated parts of chromosomes retained the

overall orientation as seen in the normal chromosomes [14]. This suggested that subchromosomal regions determine their nuclear location [14]. The differences of der(18) and der(19) were generally less pronounced than those of the normal chromosomes [15]. However, translocations do not always change the localization of chromosomal territories. Parada and coworkers reported that chromosome territories #12, 14 and 15 clustered in nuclei of normal mouse splenocytes as well as in a mouse lymphoma cell line, in which these three chromosomes were involved in two translocation events [34]. The translocation in this example did not alter the relative arrangement of the territories to each other.

A number of analyses found a correlation between the gene density of certain loci and their localization not only within the nucleus but also within their chromosomal territories. This behavior is not found in most non-clustered loci but sometimes in large regions that presumably contain active gene clusters such as the MHC cluster on chromosome 6 [10], the EDC on chromosome 1 [9] and the *MLL* gene on chromosome 11 (own data, data not shown). These loci have all been shown to be preferentially localized at the surface or even outside the surface of their territories. By plotting the gene density in 1 Mbp steps from the p to the q telomere of these chromosomes, it appeared that these genes are located in regions of high gene density (data not shown). During the course of this work, a potential contradiction between the localization of gene-dense regions at the surface of chromosomal territories and towards the center of the nucleus became apparent. This contradiction can only be solved if one assumes that actively transcribed and/or gene-dense regions loop out of territories preferentially towards the center of the nucleus.
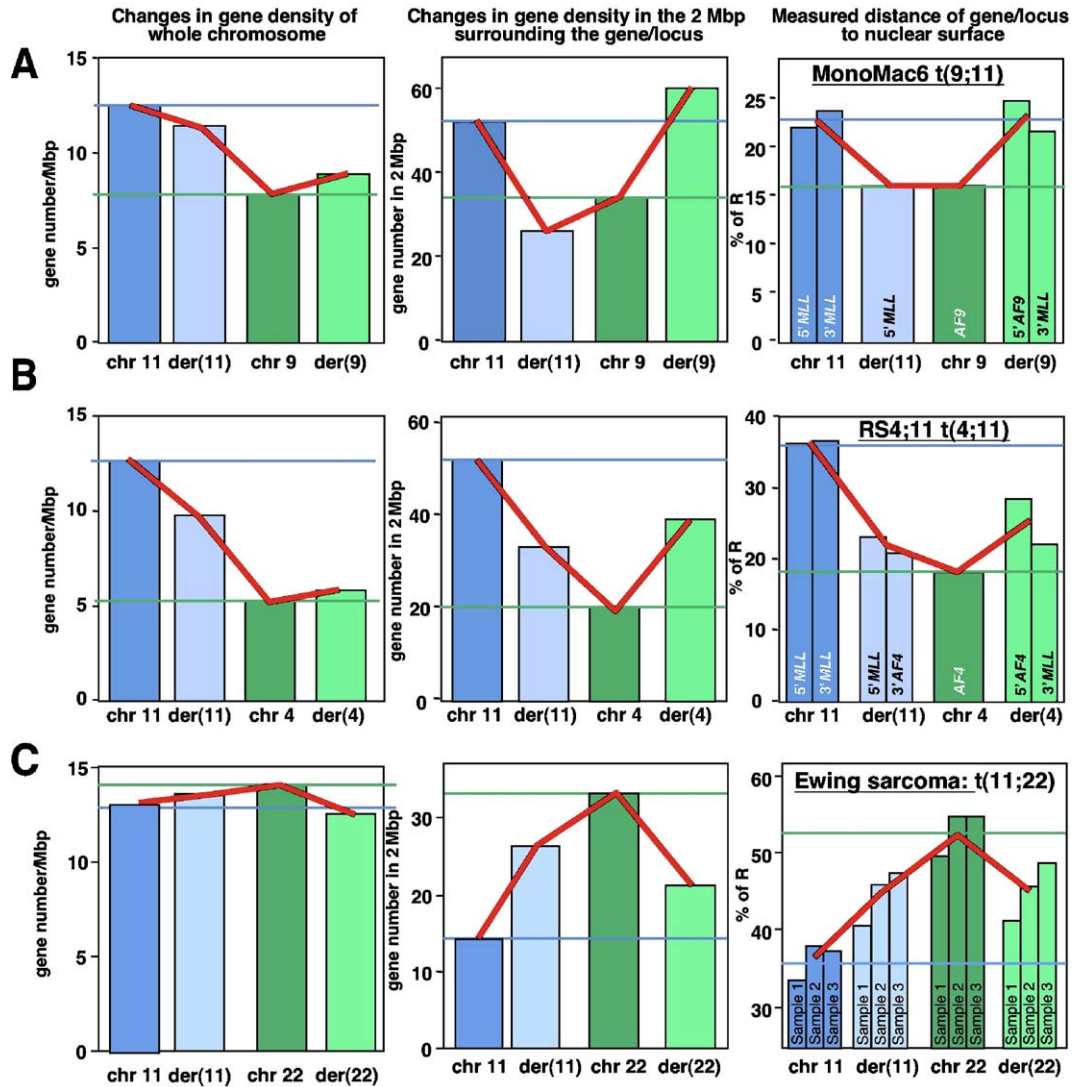
Fig. 7. Comparison of gene density of entire chromosomes with the local gene density in a 2 Mbp window surrounding the gene as a predictor for changes of 3D localization after translocation events. Dark blue column: chr 11; light blue column: der(11); dark green column: other normal chromosome; light green column: other derivative chromosome. Left panels: gene density of whole chromosomes. Center panels: gene density in the 2 Mbp window surrounding the gene. Right panels: measured distances of genes to nuclear surface. (A) Values relevant for the cell line MonoMac6 with t(9;11) involving *AF9* and *MLL*. (B) Values relevant for the cell line RS4;11 with t(4;11) involving *AF4* and *MLL*. (C) Values relevant for a literature example: translocation t(11;22) involving the genes *EWSR1* on chr 22 and *FLI1* on chr 11 of Ewing sarcoma cells. The data were taken from published 2D image analysis [27]. Original data were converted from distances of signals to nuclear center in percent of total radius to distances of signals to nuclear periphery. Average distance values are displayed. Gene density information was obtained from the website http://www.ncbi.nlm.nih.gov/mapview/maps.cgi and calculated for the derivative chromosomes. chr = normal chromosome. der = derivative chromosome. Red lines indicate the general pattern of change between the normal and derivative chromosomes.

In fact, close inspection of some published results seems to indicate that this is the case. The majority of images show genes looping out of territories towards the center of the nucleus [9–11,13]. What determines the position of a sequence within the nucleus and what could be the mechanisms that maintain a gradient of gene density from the nuclear surface to the nuclear center? Published work suggests that, at the chromatin level, the more gene-dense regions of the genome localize to the nuclear interior, and the more gene-poor chromatin locates at the nuclear periphery [17,35]. Our work now suggests that the local gene density of a 2 Mbp window surrounding a gene seems to be a good predictor for the nuclear position of genes. However, gene density alone cannot be the determining factor because of cell-type-specific differences we have observed. Furthermore, it has been shown that genes change position after activation or inactivation [36], a process which does not alter the actual gene content. Nevertheless, the gene density that surrounds *MLL* and its translocation partners correlates remarkably well with their 3D position in the nucleus. It is likely that the transcriptional activity of loci contributes to their localization. The more genes are present in a local region, the higher the potential transcriptional activity could be.

To determine whether this novel method can also be applied more generally to predict the location of subchromosomal domains, published data on the location of telomeres were reanalyzed. Weierich et al. reported that the location of the telomeres was very different between mouse and human [37]. Mouse telomeres clustered more in the nuclear periphery than human telomeres. This result could not have been predicted from the general gene density of the entire chromosomes from mouse and human since the median densities are quite similar (red lines in Figs. 8A and B). However, when the gene densities of only the last 2 Mbp of each telomere were considered, the median number of genes present in mouse was much lower (1.5) than in humans (14.25) (Figs. 8C and D), whereas the mean gene density of all chromosomes in both species was similar. One could argue that mouse chromosomes are acrocentric, but even if only q telomeres are considered, again, many fewer genes are found in the 2 Mbp window of the q telomeres of mouse (18 genes) than of humans (34.5 genes). The analysis therefore demonstrates that local gene densities can allow a more accurate prediction of 3D localization of not only genes but also chromosomal domains than the total chromosomal gene density.

It was speculated that centromeres might be important for the chromosome position. After centromeric heterochromatin was disrupted with a DNA interchelator, positioning patterns

of chromosomes were lost [38]. It was therefore assumed that chromosome-specific timing of sister chromatid separation transmits the position of a chromosome from one cell generation to the next. If the centromere of chromosome 11 would be the determining factor of its position, 5′MLL in the der(11) should have maintained the same position as in the normal chromosome 11, which is clearly not the case. If the telomeres played a significant role in the position, 3′MLL should have the same position in der(4) and in normal chromosome 11, and that is not the case either.

A positional change caused by a translocation event was not only observed for whole chromosomes. A distinct change in the position of genes (EWSR1 on chromosome 11 and FLI1 on chromosome 20) was observed after their reciprocal translocation [27]. Normal EWSR1 had a more central, FLI1 a more peripheral position. Both fusion genes took a position intermediate for both normal genes. This finding was interpreted to be caused by the changed gene density of the translocated chromosomes. Consistent with this model, it was found that the two genes ABL1 (on chromosome 9) and BCR (on chromosome 22) did not significantly change their position after translocation (formation of the Philadelphia chromosome) because the position of these genes on the normal chromosomes was very similar. It was proposed that the radial location of the fusion gene does not depend on the location of the
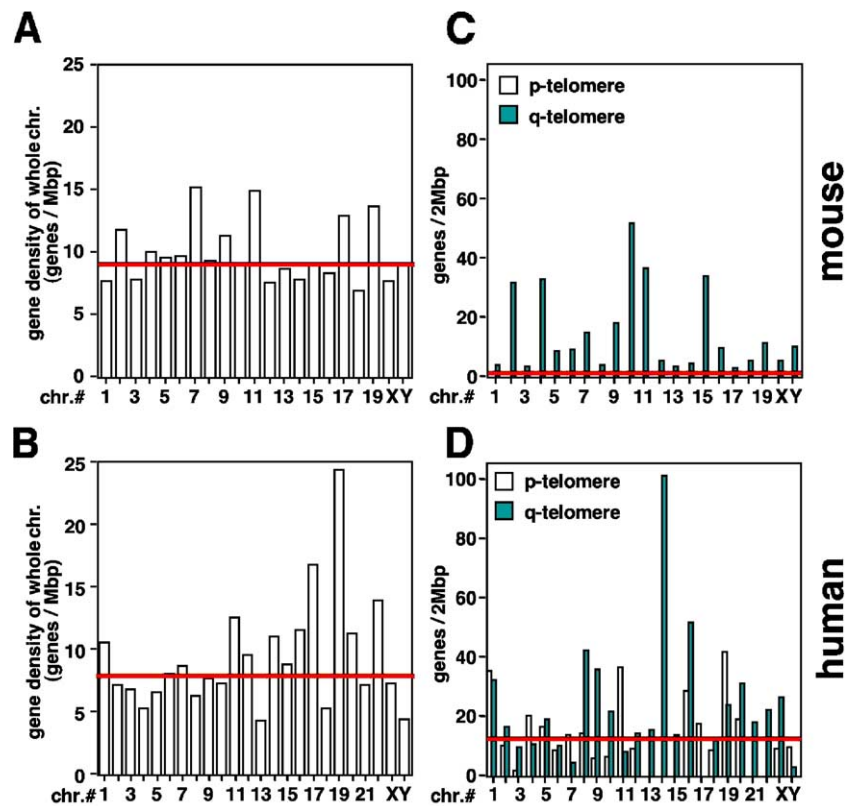

Fig. 8. Human and mouse telomeres acquire very different 3D nuclear positions due to different local gene densities. (A, B) Gene density of entire chromosomes of mouse (A) and human (B). Median gene density (red lines) is 9.0 genes/Mbp for mouse chromosomes and 7.9 for human chromosomes. (C, D) Gene density in the terminal 2 Mbp or each telomere in mouse (C) and human (D). The median number of genes (red lines) found in this window was 1.5 genes for mouse and 14.3 genes for human.

translation event but that it might be determined by the final structure of the chimeric chromosomes [27]. Our analysis now suggests that it is the local gene density surrounding a gene that determines its 3D localization in the nucleus.

The *MLL* gene has a certain probability of localization relative to the nuclear surface. In addition, during FISH analysis of peripheral blood and 7 hematopoietic cell lines, it appeared often at the surface or even outside of the stainable territory of chromosome 11 (data not shown). This could be relevant for *MLL*'s propensity to be a major translocation hotspot [39,40]. This localization seems to be characteristic of *MLL* since a control gene, *AF9*, had a more internal localization. The analysis indicated that, in the majority of the hematopoietic cells, *MLL* including the 3′ chromosomal regions adjacent to *MLL* is located at the surface or outside of the stainable chromosome 11 territory.

Although *MLL* and its translocation partners were found to have a preferred distance to the nuclear surface, the position of these genes within the predicted shells was random. Using angle measurements, no evidence was found for a clustered or polarized organization of genes (data not shown). This concurs with the assumption that chromosome positioning patterns are probabilistic rather than absolute [41].

The results of this work have the potential to shed a new light on the mechanism and the effects of reciprocal translocations. So far, the concept of a reciprocal translocation is that two genes get disrupted leading to the loss or gain of function mutations. If these genes are part of a signal transduction cascade, the expression and activity of many other genes can also be influenced. After a change in position, genes in close proximity of the breakpoint, not disrupted by the break itself, could also be affected by the positional change resulting in a change in their expression. One could speculate that a shift to the nuclear surface would result in downregulated transcriptional activity and a shift to the nuclear interior could upregulate the expression of genes, which could contribute to cellular transformation.

Appendix A. Supplementary data

Supplementary data associated with this article can be found in the online version at doi:10.1016/j.yexcr.2005.07.020.

References

[1] J.D. Rowley, The role of chromosome translocations in leukemogenesis, Semin. Hematol. 36 (1999) 59–72.

[2] B.J. Druker, C.L. Sawyers, R. Capdeville, J.M. Ford, M. Baccarani, J.M. Goldman, Chronic myelogenous leukemia, Hematology (Am. Soc. Hematol. Educ. Program) (2001) 87–112.

[3] J. Huret, 11q23 rearrangements in leukaemia, Atlas Genet. Cytogenet. Oncol. Haematol. (2003 August) http://www.infobiogen.fr/services/chromcancer/Anomalies/11q23ID1030.html.

[4] S. Ziemin-van der Poel, N.R. McCabe, H.J. Gill, R. Espinosa III, Y. Patel, A. Harden, P. Rubinelli, S.D. Smith, M.M. LeBeau, J.D. Rowley, et al., Identification of a gene, MLL, that spans the breakpoint in 11q23 translocations associated with human leukemias, Proc. Natl. Acad. Sci. U. S. A. 88 (1991) 10735–10739.

[5] R. Marschalek, I. Nilson, K. Lochner, R. Greim, G. Siegler, J. Greil, J.D. Beck, G.H. Fey, The structure of the human ALL-1/MLL/HRX gene, Leuk. Lymphoma 27 (1997) 417–428.

[6] J.J. Roix, P.G. McQueen, P.J. Munson, L.A. Parada, T. Misteli, Spatial proximity of translocation-prone gene loci in human lymphomas, Nat. Genet. 34 (2003) 287–291.

[7] A. Kurz, S. Lampel, J.E. Nickolenko, J. Bradl, A. Benner, R.M. Zirbel, T. Cremer, P. Lichter, Active and inactive genes localize preferentially in the periphery of chromosome territories, J. Cell Biol. 135 (1996) 1195–1205.

[8] S. Dietzel, K. Schiebel, G. Little, P. Edelmann, G.A. Rappold, R. Eils, C. Cremer, T. Cremer, The 3D positioning of ANT2 and ANT3 genes within female X chromosome territories correlates with gene activity, Exp. Cell Res. 252 (1999) 363–375.

[9] R.R. Williams, S. Broad, D. Sheer, J. Ragoussis, Subchromosomal positioning of the epidermal differentiation complex (EDC) in keratinocyte and lymphoblast interphase nuclei, Exp. Cell Res. 272 (2002) 163–175.

[10] E.V. Volpi, E. Chevret, T. Jones, R. Vatcheva, J. Williamson, S. Beck, R.D. Campbell, M. Goldsworthy, S.H. Powis, J. Ragoussis, J. Trowsdale, D. Sheer, Large-scale chromatin organization of the major histocompatibility complex and other regions of human chromosome 6 and its response to interferon in interphase nuclei, J. Cell Sci. 113 (2000) 1565–1576.

[11] N.L. Mahy, P.E. Perry, W.A. Bickmore, Gene density and transcription influence the localization of chromatin outside of chromosome territories detectable by FISH, J. Cell Biol. 159 (2002) 753–763.

[12] M.O. Scheuermann, J. Tajbakhsh, A. Kurz, K. Saracoglu, R. Eils, P. Lichter, Topology of genes and nontranscribed sequences in human interphase nuclei, Exp. Cell Res. 301 (2004) 266–279.

[13] N.L. Mahy, P.E. Perry, S. Gilchrist, R.A. Baldock, W.A. Bickmore, Spatial organization of active and inactive genes and noncoding DNA within chromosome territories, J. Cell Biol. 157 (2002) 579–589.

[14] J.A. Croft, J.M. Bridger, S. Boyle, P. Perry, P. Teague, W.A. Bickmore, Differences in the localization and morphology of chromosomes in the human nucleus, J. Cell Biol. 145 (1999) 1119–1131.

[15] M. Cremer, K. Kupper, B. Wagler, L. Wizelman, J. von Hase, Y.

Weiland, L. Kreja, J. Diebold, M.R. Speicher, T. Cremer, Inheritance of gene density-related higher order chromatin arrangements in normal and tumor cell nuclei, J. Cell Biol. 162 (2003) 809–820.

[16] H.B. Sun, J. Shen, H. Yokota, Size-dependent positioning of human chromosomes in interphase nuclei, Biophys. J. 79 (2000) 184–190.

[17] A. Bolzer, G. Kreth, I. Solovei, D. Koehler, K. Saracoglu, C. Fauth, S. Muller, R. Eils, C. Cremer, M.R. Speicher, T. Cremer, Three-dimensional maps of all chromosomes in human male fibroblast nuclei and prometaphase rosettes, PLoS Biol. 3 (2005) e157.

[18] M. Cremer, J. von Hase, T. Volm, A. Brero, G. Kreth, J. Walter, C. Fischer, I. Solovei, C. Cremer, T. Cremer, Non-random radial higher-order chromatin arrangements in nuclei of diploid human cells, Chromosome Res. 9 (2001) 541–567.

[19] S. Boyle, S. Gilchrist, J.M. Bridger, N.L. Mahy, J.A. Ellis, W.A. Bickmore, The spatial organization of human chromosomes within the nuclei of normal and emerin-mutant cells, Hum. Mol. Genet. 10 (2001) 211–219.

[20] M. Scheuermann, Characterization of nuclear subcompartments by analysis of the topology of genes and non-transcribed sequences as well as ectopically expressed proteins in mammalian cells with different karyotypes. Dissertation, submitted to the Combined Faculties for the Natural Sciences and for Mathematics of the Ruperto-Carola University of Heidelberg, Germany for the degree of Doctor of Natural Sciences, (2004).

[21] J.M. Bridger, S. Lampel, P. Lichter, Subcellular localization of genes and their products: Section 12. In situ hybridization, in: D.L. Spector, R.D. Goldman, A.L. Leinwand (Eds.), Cells: A Laboratory Manual, 1998.

[22] A. Eggen, M. Gautier, A. Billaut, E. Petit, H. Hayes, P. Laurent, C. Urban, M. Pfister-Genskow, K. Eilertsen, M.D. Bishop, Construction and characterization of a bovine BAC library with four genome-equivalent coverage, Genet. Sel. Evol. 33 (2001) 543–548.

[23] P. Lichter, A.L. Boyle, T. Cremer, D.C. Ward, Analysis of genes and chromosomes by nonisotopic in situ hybridization, Genet. Anal. Tech. Appl. 8 (1991) 24–35.

[24] J. Gao, A.E. Murmann, J.D. Rowley, P. Lichter, R. Eils, Three-dimensional quantitative tools to analyze the spatial arrangement of translocation partner gene, (in preparation).

[25] Y. Jin, F. Mertens, K. Arheden, N. Mandahl, J. Wennerberg, M. Dictor, S. Heim, F. Mitelman, Karyotypic features of malignant tumors of the nasal cavity and paranasal sinuses, Int. J. Cancer 60 (1995) 637–641.

[26] L.A. Parada, P.G. McQueen, T. Misteli, Tissue-specific spatial organization of genomes, Genome Biol. 5 (2004) R44.

[27] R. Taslerova, S. Kozubek, E. Lukasova, P. Jirsova, E. Bartova, M. Kozubek, Arrangement of chromosome 11 and 22 territories, EWSR1 and FLI1 genes, and other genetic elements of these chromosomes in human lymphocytes and Ewing sarcoma cells, Hum. Genet. 112 (2003) 143–155.

[28] H. Yokota, M.J. Singer, G.J. van den Engh, B.J. Trask, Regional differences in the compaction of chromatin in human G0/G1 interphase nuclei, Chromosome Res. 5 (1997) 157–166.

[29] H. Yokota, G. van den Engh, J.E. Hearst, R.K. Sachs, B.J. Trask, Evidence for the organization of chromatin in megabase pair-sized loops arranged along a random walk path in the human G0/G1 interphase nucleus, J. Cell Biol. 130 (1995) 1239–1249.

[30] S. Kozubek, E. Bartova, M. Kozubek, E. Lukasova, A. Cafourkova, I. Koutna, M. Skalnikova, Spatial distribution of selected genetic loci in nuclei of human leukemia cells after irradiation, Radiat. Res. 155 (2001) 311–319.

[31] I. Solovei, A. Cavallo, L. Schermelleh, F. Jaunin, C. Scasselati, D. Cmarko, C. Cremer, S. Fakan, T. Cremer, Spatial preservation of nuclear chromatin architecture during three-dimensional fluorescence in situ hybridization (3D-FISH), Exp. Cell Res. 276 (2002) 10–23.

[32] J.M. Bridger, S. Boyle, I.R. Kill, W.A. Bickmore, Re-modelling of nuclear architecture in quiescent and senescent human fibroblasts, Curr. Biol. 10 (2000) 149–152.

[33] H. Tanabe, S. Muller, M. Neusser, J. von Hase, E. Calcagno, M. Cremer, I. Solovei, C. Cremer, T. Cremer, Evolutionary conservation of chromosome territory arrangements in cell nuclei from higher primates, Proc. Natl. Acad. Sci. U. S. A. 99 (2002) 4424–4429.

[34] L.A. Parada, P.G. McQueen, P.J. Munson, T. Misteli, Conservation of relative chromosome positioning in normal and cancer cells, Curr. Biol. 12 (2002) 1692–1697.

[35] C. Federico, S. Saccone, L. Andreozzi, S. Motta, V. Russo, N. Carels, G. Bernardi, The pig genome: compositional analysis and identification of the gene-richest regions in chromosomes and nuclei, Gene 343 (2004) 245–251.

[36] S.T. Kosak, J.A. Skok, K.L. Medina, R. Riblet, M. Le, M. Beau, A.G. Fisher, H. Singh, Subnuclear compartmentalization of immunoglobulin loci during lymphocyte development, Science 296 (2002) 158–162.

[37] C. Weierich, A. Brero, S. Stein, J. von Hase, C. Cremer, T. Cremer, I. Solovei, Three-dimensional arrangements of centromeres and telomeres in nuclei of human and murine lymphocytes, Chromosome Res. 11 (2003) 485–502.

[38] D. Gerlich, J. Beaudouin, B. Kalbfuss, N. Daigle, R. Eils, J. Ellenberg, Global chromosome positions are transmitted through mitosis in mammalian cells, Cell 112 (2003) 751–764.

[39] P.A. Futreal, L. Coin, M. Marshall, T. Down, T. Hubbard, R. Wooster, N. Rahman, M.R. Stratton, A census of human cancer genes, Nat. Rev., Cancer 4 (2004) 177–183.

[40] H.G. Drexler, H. Quentmeier, R.A. MacLeod, Malignant hematopoietic cell lines: in vitro models for the study of MLL gene alterations, Leukemia 18 (2004) 227–232.

[41] L.A. Parada, J.J. Roix, T. Misteli, An uncertainty principle in chromosome positioning, Trends Cell Biol. 13 (2003) 393–396.